Dalton Transactions

Accepted Manuscript

ROYAL SOCIETY OF CHEMISTRY

www.rsc.org/dalton

Journal Name

ARTICLE

Construction of $Ni^{II}Ln^{III}M^{III}$ (Ln = Gd^{III}, Tb^{III}; M = Fe^{III}, Cr^{III}) Clusters Showing Slow Magnetic Relaxations

Received 00th January 20xx,
Accepted 00th January 20xx

DOI: 10.1039/x0xx00000x

www.rsc.org/

Chao Chen,[a] Yashu Liu,[b] Ping Li,[a] Hongbo Zhou[a] and Xiaoping Shen*[a]

Four heterotrimetallic 3d-3d'-4f complexes, $[Ni(L)Gd(H_2O)_4][Cr(CN)_6]CH_3OH{\cdot}2H_2O$ (**1**), $[Ni(L)Tb(H_2O)_4][Cr(CN)_6]CH_3OH{\cdot}2H_2O$ (**2**), $[Ni(L)Gd(H_2O)_4][Fe(CN)_6]{\cdot}3H_2O$ (**3**) and $[Ni(L)Tb(H_2O)_4][Fe(CN)_6]CH_3OH{\cdot}2H_2O$ (**4**) (H_2L = N,N-ethylenebis(3-methoxysalicylaldiimine)) were synthesized and characterized structurally and magnetically. The X-Ray structural analysis revealed that these complexes are isostructural, in which $Ni^{II}Ln^{III}M^{III}$ (Ln = Tb^{III}, Gd^{III}; M = Fe^{III}, Cr^{III}) is arranged in trinuclear clusters. Then, these clusters further interact with each other via weak hydrogen bonds to form the high dimensional supramolecular networks. Magnetic investigation indicates that the Ni(II) centers are diamagnetic. Dominant antiferromagnetic coupling is presented in complexes **1** and **3**. An AC magnetic susceptibility measurement indicates that complexes **2** and **4** show typical field induced slow magnetic relaxation, which might be caused by the magnetic anisotropy of center Tb^{III} ions

INTRODUCTION

The single molecule magnet (SMM)[1] and single chain magnet (SCM)[2] are one of the hottest topics in the research field of molecule magnetism due to their potential applications in magnetic devices and quantum computers, *etc*. In these researches, the 3d transitional metal ions such as Cr, Mn, Fe, Co, Ni, Cu, etc. are often employed to construct such materials. In particular, the magnetic anisotropy brought by Mn^{III}, Fe^{III} and Co^{II} was proved to be important for the SMM or SCM behaviors.[3-5] At the same time, the paramagnetic lanthanide metals have also attracted much attention because of their high spin values and large magnetic anisotropy.[1c] As a representative work, J. R. Long and coworkers reported the SMM of $\{[(Me_3Si)_2N]_2(THF)Ln\}_2(\mu\text{-}\eta^2\text{:}\eta^2\text{-}N_2)^-$ (Ln = Tb, Ho, Er) with recorded high block temperature (T_B = 14 K).[6] It was found that the magnetic anisotropy of Ln^{III} is affected by the coordination environment, which is very interesting and stimulates the research enthusiasm for the so-called single ion magnet (SIM).[7] Even so, the family of polynuclear lanthanide metals complexes has the dominant position in the research field because of their interesting topological structures and magnetism. One of the branches of the research is the d-f assemblies in which the 3d/4d/5d and 4f metals are combined together to design SMMs and SCMs.[1c,2d,2e,2f,8] Though the d-f magnetic complexes have been synthesized and characterized since the beginning of this century, the example of d-f based SMMs and SCMs are still scarle.[1c] Such a fact implies that the study on the 3d-4f magnetic systems is still at its early stage and deserves to be further explored. The advantages of the d-f magnetic assemblies can be concluded as following: (1) The system provides a broad space for researchers to design special molecular structures and tune the magnetic properties. (2) The Ln^{III} ions could produce significant magnetic anisotropy when the coordination field is reasonably controlled, as demonstrated by SIM.[7] (3) The molecular overall magnetic anisotropy can be further enhanced by the exchange coupling between 3d and 4f spin carriers. Elegant example to this category is the $\{Dy_2Cr_2\}$ SMM with blocking temperature of 3.7 K reported by S. K. Langley *et al*.[9] This study highlights the essential role played by d-f combined systems in designing new SMMs with improved properties.

Against this background, the magnetic assemblies based on d-f combined systems are under investigation in our laboratory, and we have recently obtained new examples of heterotrimetallic 3d-3d'-4f complexes using the compartmental Schiff base ligand of H_2L (H_2L = N,N-ethylenebis(3-methoxysalicylaldiimine)). Though some relevant 3d-3d'-4f complexes such as CoCuLn,[10] CrCoLn,[11] CrCuLn,[10a,10c,10d,12] FeCuLn,[10,13] FeNiLn,[14] NiCuLn[15] were reported previously, there are still some systems that are not investigated up to now. To the best of our knowledge, there are no reports for the CrFeLn, CrMnLn, CrNiLn, FeCoLn, MnCuLn, MnNiLn complexes. Therefore, this field indeed deserves to further explore. In this paper, we report the first examples of CrNiLn complexes with formulas of $[Ni(L)Gd(H_2O)_4][Cr(CN)_6]CH_3OH{\cdot}2H_2O$ (**1**) and

[a] School of Chemistry and Chemical Engineering, Jiangsu University, Zhenjiang 212013, China. E-mail: Hxiaopingshen@163.com
[b] School of Environmental and Chemical Engineering, Jiangsu University of Science and Technology, Zhenjiang 212003, China

Electronic Supplementary Information (ESI) available: Crystallographic data (CCDC 1401613, **1**; 1401614, **2**; 1420594, **3**, 1420595, **4**), additional synthetic, structural and magnetic details. For ESI and crystallographic data in CIF or other electronic format. See DOI: 10.1039/x0xx00000x

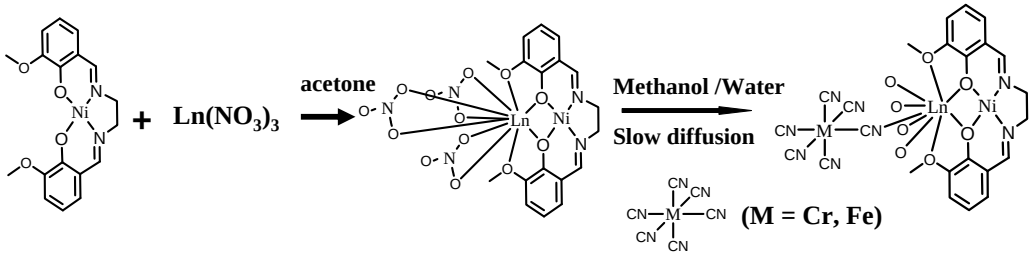

Scheme 1. Construction of heterotrimetallic 3d-3d'-4f magnetic complexes via a two-step approach with the assistance of the compartmental Schiff base ligand of H_2L.

$[Ni(L)Tb(H_2O)_4][Cr(CN)_6]CH_3OH{\cdot}2H_2O$ (**2**), together with two additional FeNiLn examples of $[Ni(L)Gd(H_2O)_4][Fe(CN)_6]{\cdot}3H_2O$ (**3**) and $[Ni(L)Tb(H_2O)_4][Fe(CN)_6]CH_3OH{\cdot}2H_2O$ (**4**) (H_2L = N,N-ethylenebis(3-methoxysalicylaldiimine)). Interestingly, the $NiTb^{III}M$ (M = Cr, Fe) complexes show field induced slow magnetic relaxation behaviors.

EXPERIMENTAL SECTION

Reagents and Materials

All the chemicals and solvents in this work are reagent grade and used as received without further purification. The $Ni^{II}(L){\cdot}H_2O$ and $[Ni(L)Ln](NO_3)_3$ (Ln = Gd, Dy) precursors were synthesized according to the literature method.[16]

Syntheses of the Complexes

$[Ni(L)Gd(H_2O)_4][Cr(CN)_6]CH_3OH{\cdot}2H_2O$ (**1**) A methanol solution (10 mL) of the prepared $[Ni(L)Gd](NO_3)_3$ (0.1 mmol) was diffused slowly into a an aqueous solution (10 mL) of $K_3Cr(CN)_6$ (0.1 mmol) through a H-shaped tube, and the block red crystals of **1** suitable for X-ray diffraction were formed in two weeks, which were collected and washed with methanol and dried in air. Anal. found: C, 33.20; H, 3.65; N, 12.60%. Calcd for $C_{25}H_{34}CrGdN_8NiO_{11}$: C, 33.72; H, 3.85; N, 12.58%. IR: ν_{max}/cm^{-1} 3406(m), 2111(m), 1623(s), 1542(m), 1469(m), 1390(m), 1290(m), 808(m), 568(m).

$[Ni(L)Tb(H_2O)_4][Cr(CN)_6]CH_3OH{\cdot}2H_2O$ (**2**) Complex **2** as block red single crystals was prepared with the same procedure as **1** except with $[Ni(L)Tb](NO_3)_3$ instead of $[Ni(L)Gd](NO_3)_3$. Anal. found: C, 33.46; H, 3.75; N, 12.50%. Calcd for $C_{25}H_{34}CrTbN_8NiO_{11}$: C, 33.65; H, 3.84; N, 12.56%. IR: ν_{max}/cm^{-1} 3417(m), 2111(m), 1614(s), 1550(m), 1469(m), 1392(m), 1290(m), 754(w), 613(m).

$[Ni(L)Gd(H_2O)_4][Fe(CN)_6]{\cdot}3H_2O$ (**3**) Complex **3** was prepared according to the same procedure of **1** by replacing $K_3Cr(CN)_6$ with $K_3Fe(CN)_6$. Anal. found: C, 32.52; H, 3.73; N, 12.48%. Calcd for $C_{24}H_{32}FeGdN_8NiO_{11}$: C, 32.74; H, 3.66; N, 12.73%. IR: ν_{max}/cm^{-1} 3405(m), 2132(m), 1621(s), 1550(m), 1473(m), 1402(m), 1243(m), 755(w), 612(m).

$[Ni(L)Tb(H_2O)_4][Fe(CN)_6]CH_3OH{\cdot}2H_2O$(**4**) Complex **4** was prepared with the same procedure as **2** by replacing $K_3Cr(CN)_6$ with $K_3Fe(CN)_6$. Anal. found: C, 33.15; H, 3.65; N, 12.35%. Calcd for $C_{25}H_{34}TbFeN_8NiO_{11}$: C, 33.51; H, 3.82; N, 12.51%. IR: ν_{max}/cm^{-1} 3415(m), 2132(m), 1618(s), 1551(m), 1475(m), 1403(m), 1243(m), 754(w), 610(m).

Physical measurements

The elemental analyses for C, H and N were performed at a Perkin-Elmer 240C analyzer. The IR spectra were recorded with a Nicolet FT-170SX spectrometer. The magnetic susceptibility of the micro-crystalline samples was measured under 100 Oe from 300 to 1.8 K on a Quantum Design MPMP-XL7 SQUID magnetometer. The field dependent magnetization was record at 1.8-5.5 K using the applied *dc* field in the range from 0 to 70 kOe. The alternating current (*ac*) susceptibility measurements were conducted at frequencies ranging from 1 to 1500 Hz with a *dc* field of 0-3000 Oe and an *ac* field amplitude of 3 Oe. Measured susceptibilities were corrected considering both the sample holder as background and diamagnetism estimated from Pascal constants.[17]

X-ray crystallography

Single crystal X-ray crystallographic diffraction data were collected at 173 K on a Bruker *SMART APEX CCD* area detector diffractometer. Graphite-monochromated Mo K_α radiation (λ = 0.71073 Å) and the φ and ω scan mode were adopted for the data collection. Diffraction data analysis and reduction were performed with the programs of *SMART*, *SAINT* and *XPREP*.[18] The structures were solved based on direct methods and refined by a full-matrix least-squares method on F^2 using the SHELXL crystallographic software package.[19] All the non-hydrogen atoms were located in difference Fourier maps and refined by anisotropic thermal parameters, while all of the hydrogen atoms were added geometrically at idealized positions, and included in the refinement of isotropical thermal parameters with the *U* values fixed using a riding model. The water-H atoms were not able to be located from the residual peaks and they were not found in the structures. Besides, the methanol molecules in **1** and **2** are not present with unit occupancy, and they were allowed an anisotropic free variable refinement with partial occupancies. Crystallographic data for **1**–**4** are summarized in Table 1.

Table 1. Details of the crystal data and structural refinement parameters of **1**–**4**.

	1	**2**	**3**	**4**
Formula	$C_{25}H_{34}CrGdN_8NiO_{11}$	$C_{25}H_{34}CrTbN_8NiO_{11}$	$C_{24}H_{32}FeGdN_8NiO_{11}$	$C_{25}H_{34}TbFeN_8NiO_{11}$
M/g mol^{-1}	890.52	892.20	880.35	896.05
Crystal system	monoclinic	monoclinic	monoclinic	monoclinic
Space group	$P2_1/c$	$P2_1/c$	$P2_1/c$	$P2_1/c$
a /Å	13.071(3)	13.051(3)	12.862(3)	12.861(3)
b /Å	12.139(2)	12.150(2)	12.012(2)	12.014(2)
c /Å	21.735(4)	21.711(4)	21.580(4)	21.577(4)
α / º	90	90	90	90.00
β /º	106.84(3)	106.89(3)	106.72(3)	106.73(3)
γ /º	90	90	90	90.00
V/Å^3	3300.8(12)	3294.0(12)	3193.1(12)	3193.0(11)
Z	4	4	4	4
d_{calc} /g cm^{-3}	1.740	1.751	1.802	1.831
F(000)	1692.5	1705	1696	1724
Collected reflections	15133	15052	14590	14367
Observed reflections	6311	6281	6111	6060
Independent reflections	5461	5650	5424	5526
R_{int}	0.0437	0.0247	0.0255	0.0266
data/restraints /parameters	6311/0/427	6281/7/424	6111/0/417	6060/6/426
GOF[c] on F^2	1.085	1.071	1.058	1.053
R_1[a] (I >2 $\sigma(I)$)	0.0497	0.0355	0.0338	0.0323
wR_2[b](all data)	0.1050	0.0409	0.0823	0.0822

[a] $R_1 = \sum||F_o| - |F_c||/\sum|F_o|$. [b] $wR_2 = [\sum w(F_o^2 - F_c^2)^2/\sum w(F_o^2)^2]^{1/2}$; $w = 1/\sigma^2(|F_o|)$. [c] Goodness of fit: GOF = $[\sum w(F_o^2 - F_c^2)^2/(n-p)]^{1/2}$, where n is the number of reflections and p is the number of parameters

RESULTS AND DISCUSSION

Syntheses and Characterization

According to previous reports, the reaction of $Ni^{II}(L)\cdot H_2O$, $Ln(NO_3)_3$ and additional hexacyanometallates can form different structures.[20] In most cases, the one-pot reaction of these precursors would produce polynuclear clusters in which the nickel atoms are involved in the coordination to hexacyanometallates, leading to the formation of interesting hexanuclear or octanuclear molecular cycles.[20a] In our present work, the reaction route was divided into two steps, as illustrated in Scheme 1, and the trinuclear clusters of **1**-**4** were formed. The relatively low nuclearity clusters of **1**-**4** might be limited by the square planar coordination geometry of low spin Ni(II) centers presented in $[Ni(L)Ln](NO_3)_3$ moities. The IR spectrums verify the structures of complexes **1** – **4**. The characteristic absorption peaks at 2100-2150 cm^{-1} can be assigned to the cyanide group, and the other absorption bands are ascribed to the characteristic absorptions of the Schiff base ligands.

Crystal Structures

The selected structural parameters such as key bond distances and angles are listed in Table S1. The crystal structures of complexes **1**-**4** are shown in Figure 1 and Figure S1 (see Supporting Information). The intermolecular short contacts and packing structures for the four complexes are shown in Figure S2.

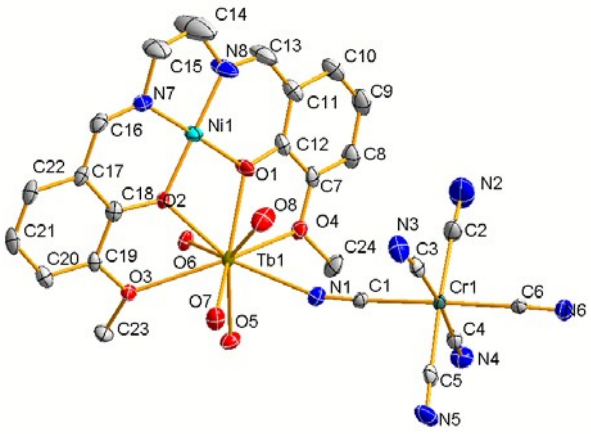

Figure 1. ORTEP (30%) diagram of asymmetric unit with selected atom-labeling scheme for complex **2**

As shown in Figure 1 and Figures S1-S2, complexes **1** - **4** are isostructural. As a representative, complex **2** is depicted in detail here. The molecular entity of **2** can be described as heterotrimetallic $Ni^{II}Tb^{III}Cr^{III}$ cluster. The Ni^{II} ion shows square coordination geometry where a pair of N, O atoms from salen-

type ligand occupies four vertex positions. The Ni-N/O bond distances (1.830(4) - 1.851(3) Å) are very close to each other, which is comparable to the bond parameters shown in mononuclear Ni^{II}(salen-type) complex.[21] The center Tb ion is nine-coordinated and adopts nonsymmetrical TbO_8N coordination sphere. Such a coordination fashion is typical for the lanthanide 4f metal ion.[1c] The Tb-$O_{phenoxo/water}$ bond distances (2.335(3)- 2.516(3) Å) are somewhat shorter than those of Tb-$O_{methoxy}$ (2.608(3)-2.663(3) Å). The bond angles of Ni1-O1-Tb1 and Ni1-O2-Tb1 are 105.81(1)° and 106.13(1)°, respectively.

The dihedral angle between the planes defined by Ni1O1O2 and Tb1O1O2 is 14.8°, which is somewhat larger than those for the 3d-4f $Ni^{II}Ln^{II}$ dinuclear complexes.[16] For the hexacyanometalates moiety, the $[Cr(CN)_6]^{3-}$ coordinates to Tb^{III} ion through one of its six cyano groups, leaving the rest cyano groups terminal. The Cr-C bond distances are in the range of 2.057(5)- 2.079(5) Å, which are typical of Cr-C bond lengths. The Tb-N_{cyano} bond distance is 2.475(4) Å, which is larger than the usual scope for 3d-N distance and coincides with typical 4f-N separations. The Cr-C-N angle is almost linear (172.6(4)-178.8(4)°) while the Tb-N-C_{cyano} angle (162.9(3)°) deviates from linearity. Moreover, the molecular plane for salen-type ligand is somewhat distorted (dihedral angles between two aromatic rings planes (C7-C12; C7-C22)) are 22.1°), which could be ascribed to the TbO_8N coordination sphere presented in the cavity of salen-type ligand. For the extended structure, the weak hydrogen bond contacts between the terminal cyano nitrogen atoms and the coordinated water molecules lead to the formation of 2-D networks along *ab* plane, which further stack layer by layer along *c* axis. (Figure S1-2)

Magnetic Properties

DC magnetic susceptibility measurements for complexes **1** - **4** were carried out on the polycrystalline sample at 100 Oe in the temperature range of 1.8–300 K (Figure 2a). At room temperature, the $\chi_M T$ values for **1** - **4** are 9.7, 12.9, 9.0 and 12.1 cm^3 K mol^{-1}, respectively, which are close to the expected values for uncoupled Ln^{III}-Cr^{III}/Fe^{III} units (Theoretical value: 9.76 cm^3 K mol^{-1} for **1**; 13.7 cm^3 K mol^{-1} for **2**; 8.25 cm^3 K mol^{-1} for **3** and 12.19 cm^3 K mol^{-1} for **4**, respectively (S_{Gd} = 7/2, S_{Cr} = 3/2, S_{Fe} = 1/2, g = 2; Tb^{III}: J = 6, g_J = 1.5)). The room temperature $\chi_M T$ values of **1** - **4** suggest that the Ni^{II} ion is diamagnetic.[16] Upon cooling, the $\chi_M T$ values for **1** and **3** keep almost constant in the high temperature region, while a continuous decrease is observed for **2** and **4**. In the very low temperature zone, the $\chi_M T$ values for **1**- **4** all show rapid decrease and reach the minimum values of 2.8, 5.7, 8.0 and 9.0 cm^3 K mol^{-1}, respectively, at 1.8 K. Considering that the Ni^{II} center is diamagnetic, complexes **1** and **3** were treated as $Gd^{III}M^{III}$ (M = Cr, Fe) dinuclear units and the Kambe's method[22] was used to fit the susceptibility data. The appropriate Hamiltonian is $H = -2JS_MS_{Gd}$ (J represents the intramolecular Gd-M coupling constant). Based on this model, the data of **1** and **3** in the whole temperature region was simulated, affording the best match parameters: J = -0.4 cm^{-1}, g = 2.0, R = 2.3×10^{-4} for **1** and J = -0.12 cm^{-1}, g = 2.1, R = 1.1×10^{-4} for **3**, respectively. The result indicates the coupling nature between Gd^{III} and M^{III} is both antiferromagnetic, which is comparable to other related Gd^{III}-M^{III} (M = Cr, Fe) bimetallic systems.[23] To verify the result, the field dependence magnetization was measured under different temperatures (Figure 2b). The experimental *M vs H* curves of complexes **1** and **3** could be well simulated (Using Magpack program)[24] based on the set of parameters extracted from the susceptibility data, further confirming the parameters obtained are reasonable. The linear increase feature of the *M-H* curve for **1** at 1.8 K implies the presence of

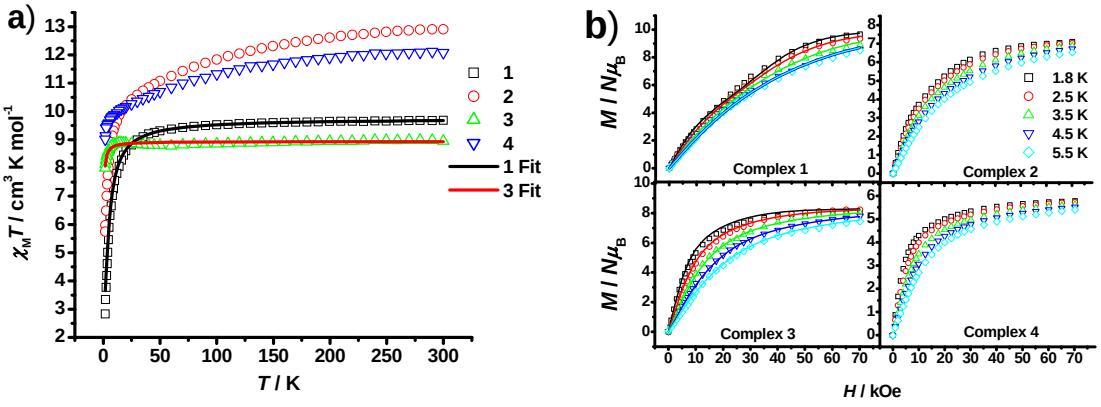

Figure 2. (a) Temperature dependence of $\chi_M T$ for **1** - **4** measured at 100 Oe. (b) Field dependence of the magnetization for **1** - **4** measured at 1.8-5.5 K. The solid lines are the best fit described in the text.

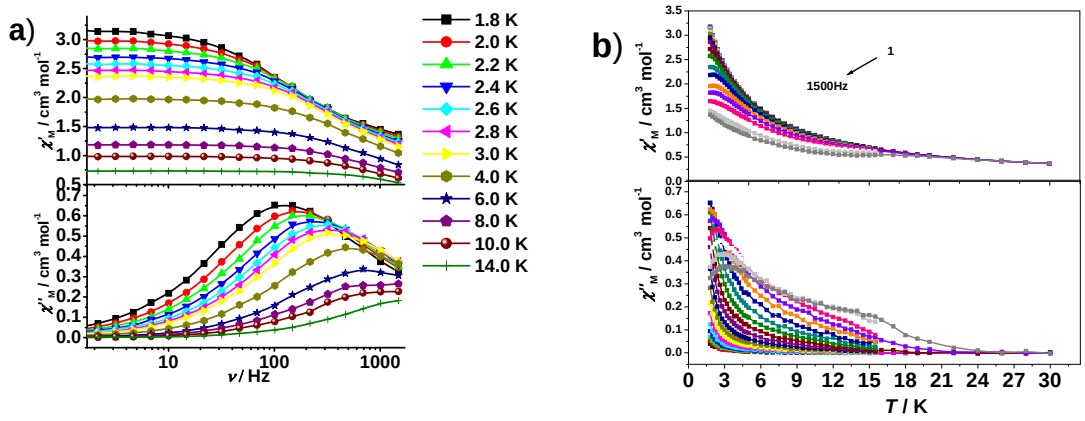

Figure 3. Frequency (a) and temperature (b) dependences of the in-phase (χ_M') and out-of-phase (χ_M'') *ac* susceptibilities of **2** in 1000 Oe *dc* field and 3 Oe *ac* field (Solid lines are guides for the eyes).

antiferromagnetic Gd^{III}- Cr^{III} state. As the *dc* field further increases, the magnetization value continuously increases and reaches the value of 9.7 $N\mu_B$ at 70 kOe. The value is close to that expected for the ferromagnetic state (10 $N\mu_B$, calculated from $M_S = g(S_{Gd}+S_{Cr})$ with $g = 2$), indicating antiferromagnetic Gd^{III}- Cr^{III} state can be overcome by strong applied *dc* field. For complex **3**, the *M-H* curves are smoother than that of **1**, indicating the Gd^{III}- Fe^{III} antiferromagnetic coupling is very weak and the system does only show paramagnetic properties. The magnetic behaviors of **1** and **3** are typical of the dinuclear metallic clusters containing isotropic spin carriers.

For **2** and **4**, the analysis of *dc* magnetic behaviors is difficult. The previous studies have revealed that the Tb^{III}-M^{III} (M = Cr, Fe) prefer to antiferromagnetic interaction.[25] Therefore, the continuous decrease of the $\chi_M T$ *vs* *T* curves of **2** and **4** upon cooling might be caused by both the intramolecular antiferromagnetic coupling and the thermal depopulation of the Stark sublevels of the 4f ion. The *M vs H* curves of **2** and **4** (Figure 2b) both reveal that the magnetizations at 70 kOe are far from saturation (12 $N\mu_B$ and 10 $N\mu_B$ for **2** and **4**, respectively, calculated from $M_S = gS(M) + gJ(Tb)$), which might be induced by the magnetic anisotropy and/or the population of low-lying excited states of Tb^{III} ions.[26] Considering that complexes **2** and **4** which contain the Tb^{III} ions might exhibit SMM behaviors, the *ac* measurement was performed. The field-dependent *ac* susceptibilities under different *dc* field (0 Oe to 3 kOe) at 1.8 K were firstly measured to verify the existence of slow magnetic relaxations (Figure S3). The result indicates that both the complexes show field induced slow magnetic relaxations when a suitable *dc* field is applied. The optimum *dc* field was determined from the field-dependent susceptibilities to be 1 kOe for **2** and 2 kOe for **4**, respectively. Such behaviors obviously indicate the presence of quantum tunneling effect in the systems that can be suppressed by the *dc* field. To study the relaxation dynamics, the frequency- and temperature dependent (Figure 3 and Figure S4) *ac* susceptibilities under fixed *dc* field (1 kOe for **2** and 2 kOe for **4**, respectively) were then measured. The result reveals that both the in-phase (χ_M') and out-of phase (χ_M'') susceptibilities of **2** and **4** are frequency- and temperature dependent. For **2**, the peaks in the frequency dependent out-of-phase (χ_M'') curves are clearly observed. The relaxation time and effective energy barrier were extracted by fitting (Figure S5) to Debye model[27] and the Arrhenius equation $\tau = \tau_0 \exp(U/k_BT)$(where τ_0 is a preexponential factor, and U is the energy barrier), affording the parameters $\tau_0 = 1.1\times10^{-4}$s, U = 3.0 cm^{-1}. The relatively small U and large τ_0 values indicate the relaxation process is significantly affected by the quantum tunneling even at the case that the *dc* field is applied. The Cole-Cole curves of **2** in the temperature range of 1.8-14 K are plotted in Figure 4. The shape of the plotted Cole-Cole curves deviates from one single semicircle, indicating the presence of different relaxation processes with different relaxation times.

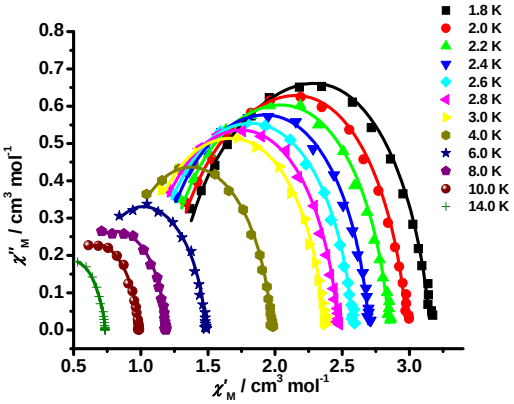

Figure 4 The Cole-Cole plots of complex **2** measured under 1 kOe *dc* field and 3 Oe *ac* field. (The solid lines are the best fits using a modified Debye model)

Indeed, the fitting of the semicircles to Debye model based on single relaxation process does not give satisfactory result. So, a modified Debye model[20a] for double relaxation process is used to fit the data of complexes **2,** giving the parameters which are listed in Table S2. For complex **4**, no peaks are detected for the frequency dependent out-of-phase (χ_M'') curves but the peaks appear in the temperature dependent out-of-phase (χ_M'')

curves. The Cole-Cole curves of complex **4** are shown in Figure S6, it can be seen that the some curves show typical V- shape, which could be assigned to be the overlap of two different relaxation process.[28a] The phenomenon that deviates from a single magnetic relaxation behavior for **2** and **4** is also observed for other Dy or Tb based SMMs[28], and could be explained by the coexistence of thermal excitation and quantum tunneling mechanism, further confirming the important role of quantum tunneling played in the magnetic relaxation at very low temperature.

Conclusions

In summary, four new examples of the complexes derived from 3d, 3d' and 4f ions have been synthesized with the assistance of a compartmental Schiff base ligand. The structural analysis reveals that these complexes show $Ni^{II}Ln^{III}M^{III}$ (M = Cr, Fe) trinuclear cluster structure. The magnetic studies reveal that complexes **1** and **3** show weak intramolecular antiferromagnetic interactions, while complexes **2** and **4** show interesting field induced slow magnetic relaxation behavior in low temperatures due to the contribution brought by anisotropic Tb^{III} ions. Considering that the relaxation behaviors of these systems are a function of both the coordination environment around the anisotropy 4f spin carriers and the magnetic coupling exchanges, their magnetic properties could be possibly improved by a rationally modification of the molecular topological structures. The related work is under way in our group.

Acknowledgements

The authors are grateful for financial support from the National Natural Science Foundation of China (No. 51072071 and 1601310042).

Notes and references

1 (a) D. Gatteschi, *Nature*, 1993, **365**, 141. (b) G. Aromi and E. K. Brechin, *Synthesis of 3d metallic single-molecule magnets*. *Struct. Bonding* (Berlin), 2006, **122**, 1. (c) H. L. C. Feltham and S. Brooker, *Coord. Chem. Rev.* 2014, **276**, 1.

2 (a) A. Caneschi, D. Gatteschi, N. Lalioti, C. Sangregorio, R. Sessoli, G. Venturi, A. Vindigni, A. Rettori, M. G. Pini and M. A. Novak, *Angew. Chem., Int. Ed.* 2001, **40**, 1760 . (b) C. Coulon, H. Miyasaka and R. Clerac, *Single-Chain Magnets: Theoretical Approach and Experimental Systems*. *Struct. Bonding* (Berlin), 2006, **122**, 163. (c) D. F. Weng, B. W. Wang, Z. M. Wang and S. Gao, *Coord. Chem. Rev.* 2013, **257**, 2484. (d) D. Visinescu, A. M. Madalan, M. Andruh, C. Duhayon, J. P. Sutter, L. Ungur, W. Van den Heuvel and L. F. Chibotaru, *Chem. Eur. J.* 2009, **15**, 11808. (e) J. Long, L. M. Chamoreau and V. Marvaud, *Dalton Trans.* 2010, **39**, 2188. (f) D. Visinescu, R. Jeon Ie, A. M. Madalan, M. G. Alexandru, B. Jurca, C. Mathoniere, R. Clerac and M. Andruh, *Dalton Trans*. 2012, **41**, 13578.

3 R. Ishikawa, R. Miyamoto, H. Nojiri, B. K. Breedlove and M. Yamashita, *Inorg Chem*. 2013, **52**, 8300

4 S. Mossin, B. L. Tran, D. Adhikari, M. Pink, F. W. Heinemann, J. Sutter, R. K. Szilagyi, K. Meyer and D. J. Mindiola, *J. Am. Chem. Soc.* 2012, **134**, 13651.

5 J. Vallejo, I. Castro, R. Ruiz-Garcia, J. Cano, M. Julve, F. Lloret, G. De Munno, W. Wernsdorfer and E. Pardo, *J. Am. Chem. Soc.* 2012, **134**, 15704.

6 J. D. Rinehart, M. Fang, W. J. Evans and J. R. Long, *J. Am. Chem. Soc.* 2011, **133**, 14236.

7 S. Cardona-Serra, J. M. Clemente-Juan, E. Coronado, A. Gaita-Arino, A. Camon, M. Evangelisti, F. Luis, M. J. Martinez-Perez and J. Sese, *J. Am. Chem. Soc.* 2012, **134**, 14982.

8 (a) H. L. Feltham, Y. Lan, F. Klower, L. Ungur, L. F. Chibotaru, A. K. Powell and S. Brooker, *Chem. Eur. J.* 2011, **17**, 4362. (b) S. Osa, T. Kido, N. Matsumoto, N. Re, A. Pochaba, J. Mrozinski, *J. Am. Chem. Soc.* 2004, 126, 420. (c) K. Q. Hu, X. Jiang, S. Q. Wu, C. M. Liu, A. L. Cui, H. Z. Kou, Dalton Trans. 2015, 44, 15413.

9 S. K. Langley, D. P. Wielechowski, V. Vieru, N. F. Chilton, B. Moubaraki, B. F. Abrahams, L. F. Chibotaru and K. S. Murray, *Angew Chem., Int Ed.* 2013, **52**, 12014.

10 (a) H. Z. Kou, B. C. Zhou and R. J. Wang, *Inorg. Chem.* 2003, **42**, 7658. (b) R. Gheorghe, M. Andruh, J. P. Costes and B. Donnadieu, *Chem. Commun.* 2003, 2778. (c) T. Shiga, A. Mishima, K. Sugimoto, H. Ōkawa, H. Oshio and M. Ohba, *Eur. J. Inorg. Chem.* 2012, 2784. (d) N. Bridonneau, G. Gontard and V.Marvaud, *Dalton Trans.* 2015, **44**, 5170.

11 T. Shiga, H. Okawa, S. Kitagawa and M. Ohba, *J. Am. Chem. Soc.* 2006, **128**, 16426.

12 (a) H. Z. Kou, K. Q. Hu, H. Y. Zhao, J. Tang and A. L. Cui, *Chem. Commun.* 2010, **46**, 6533. (b) H. Z. Kou, B. C. Zhou, S. Gao and R. Wang, *Angew. Chem., Int. Ed.* 2003, **42**, 3288. (c) R. Gheorghe, P. Cucos, M. Andruh, J. P. Costes, B. Donnadieu and S. Shova, *Chem. Eur. J.* 2006, **12**, 187.

13 (a) T. Gao, P. F. Yan, G. M. Li, J. W. Zhang, W. B. Sun, M. Suda and Y. Einaga, *Solid State Sciences*, 2010, **12**, 597. (b) J. Jankolovits, J. W. Kampf, S. Maldonado and V. L. Pecoraro, *Chem. Eur. J.* 2010, **16**, 6786. (c) R. Gheorghe, A. M. Madalan, J P. Costes, W. Wernsdorfer and M. Andruh, *Dalton Trans.* 2010, **39**, 4734. (d) W. B. Sun, P. F. Yan, G. M. Li, T. gao, M. Suda and Y. Einaga, *Inorg. Chem. Commun.* 2010, **13**, 171.

14 (a) A. Chakraborty, P. Bag, E. Riviere, T. Mallah and V. Chandrasekhar, *Dalton Trans.* 2014, **43**, 8921. (b) M. X. Yao, Q. Zheng, K. Qian, Y. Song, S. Gao and J. L. Zuo, *Chem. Eur. J.* 2013, **19**, 294.

15 (a) N. Yoshinari, A. Igashira-Kamiyama and T. Konno, *Chem. Eur. J.* 2010, **16**, 14247. (b) A. M. Madalan, N. Avarvari, M. Fourmigue, R. Clerac, L. F. Chibotaru, S. Clima and M. Andruh, *Inorg. Chem.* 2008, **47**, 940. (c) N. Bridonneau, L. M. Chamoreau, P. P. Laine, W. Wernsdorfer and V. Marvaud, *Chem. Commun.* 2013, **49**, 9476.

16 R. Koner, H. H. Lin, H. H. Wei and S. Mohanta, *Inorg. Chem.* 2005, **44,** 3524.

17 O. Kahn, *Molecular Magnetism*, VCH Publishers, New York, 1993.

18 Bruker, *SMART, SAINT and XPREP: Area Detector Control and Data Integration and Reduction Software, Bruker Analytical X-ray Instruments Inc.* Madison, Wisconsin, USA, 1995.

19 G. M. Sheldrick, *SHELXL-97*: *Program for the Refinement of Crystal Structure*; University of Göttingen: Göttingen, Germany, 1997.
20 (a) K. Q. Hu, X. Jiang, S. Q. Wu, C. M. Liu, A. L. Cui and H. Z. Kou, *Inorg. Chem.* 2015, **54**, 1206. (b) M. G. Alexandru, D. Visinescu, M. Andruh, N. Marino, D. Armentano, J. Cano, F. Lloret and M. Julve, *Chem. Eur. J.* 2015, **21**, 5429. (c) S. Dhers, J. P. Costes, P. Guionneau, C. Paulsen, L. Vendier and J. P. Sutter, *Chem. Commun.* 2015, *51*, 7875. (d) M. X. Yao, Q. Zheng, K. Qian, Y. Song, S. Gao and J. L. Zuo, *Chem. Eur. J.* 2013, **19**, 294.
21 M. A. Siegler and M. Lutz, *Cryst. Growth Des.* 2009, **9**, 1194.
22 K. Kambe, *J. Phys. Soc. Jpn.* 1950, **5**, 48.
23 (a) H. Z. Kou, S. Gao, C. H. Li, D. Z. Liao, B. C. Zhou, R. J. Wang and Y. Li, *Inorg. Chem.* 2002, **41**, 4756. (b) S. A. Stoian, C. Paraschiv, N. Kiritsakas, F. Lloret, E. Munck, E. L. Bominaar and M. Andruh, *Inorg. Chem.* 2010, **49**, 3387.
24 (a) J. J. Borras-Almenar, J. M. Clemente-Juan, E. Coronado and B. Tsukerblat, *Inorg. Chem*. 1999, **38**, 6081. (b) J. J. Borras-Almenar, J. M. Clemente-Juan, E. Coronado and B. Tsukerblat, MAGPACK, Magnetic Properties Analysis Package for Spin Clusters, version 00.1, 2000. (c) J. J. Borras-Almenar, J. M. Clemente-Juan, E. Coronado and B. J. Tsukerblat, *Comput. Chem.* 2001, **22**, 985.
25 (a) M. Estrader, J. Ribas, V. Tangoulis, X. Solans, M. Font-Bardia, M. Maestro and C. Diaz, *Inorg. Chem.* 2006, **45**, 8239. (b) A. Figuerola, J. Ribas, D. Casanova, M. Maestro, S. Alvarez and C. Diaz, *Inorg. Chem.* 2005, **44**, 6949.
26 R. Sessoli and A. K. Powell, *Coord. Chem. Rev.* 2009, **253**, 2328.
27 (a) K. S. Cole and R. H. J. Cole, *J. Chem. Phys*. 1941, **9**, 341. (b) C. J. F. Boettcher, *Theory of Electric Polarisation*, Elsevier, Amsterdam, 1952.
28 (a) S. K. Langley, N. F. Chilton, B. Moubaraki and K. S. Murray, *Inorg. Chem.* 2013, **52**, 7183. (b) L. B. Escobar, G. P. Guedes, S. Soriano, N. L. Speziali, A. K. Jordao, A. C. Cunha, V. F. Ferreira, C. Maxim, M. A. Novak, M. Andruh and M. G. Vaz, *Inorg. Chem.* 2014, **53**, 7508.

Several new 3d-3d'-4f clusters, $Ln^{III}Ni^{II}M^{III}$ (Ln = Gd, Tb; M = Fe, Cr) which show slow magnetic relaxations were presented.